HHS Public Access

Author manuscript

Cell Rep. Author manuscript; available in PMC 2019 March 19.

Published in final edited form as:

Cell Rep. 2018 December 11; 25(11): 2992–3005.e5. doi:10.1016/j.celrep.2018.11.056.

Heterogeneous Responses of Hematopoietic Stem Cells to Inflammatory Stimuli are Altered with Age

Mati Mann[1,5,6,*], **Arnav Mehta**[1,2,5], **Carl G. de Boer**[3,5], **Monika S. Kowalczyk**[3,5], **Kevin Lee**[1], **Pearce Haldeman**[1], **Noga Rogel**[3], **Abigail R. Knecht**[3], **Daneyal Farouq**[3], **Aviv Regev**[3,4,**], and **David Baltimore**[1,***]

[1]Division of Biology and Biological Engineering, California Institute of Technology, Pasadena, CA 91125, USA

[2]David Geffen School of Medicine, UCLA, Los Angeles, CA 90025, USA

[3]Broad Institute of MIT and Harvard, Cambridge, MA 02142, USA

[4]Howard Hughes Medical Institute, Koch Institute of Integrative Cancer Biology, Department of Biology, Massachusetts Institute of Technology, Cambridge, Massachusetts 02140, USA

[5]These authors contributed equally to this work

[6]Lead contact. mati@caltech.edu

Summary

Long-term hematopoietic stem cells (LT-HSCs) maintain hematopoietic output throughout an animal's lifespan. However, with age the balance is disrupted and LT-HSCs produce a myeloid-biased output, resulting in poor immune responses to infectious challenge and the development of myeloid leukemias. Here, we show that young and aged LT-HSCs respond differently to inflammatory stress, such that aged LT-HSCs produce a cell-intrinsic, myeloid-biased expression program. Using single-cell RNA-seq, we identify a myeloid-biased subset within the LT-HSC population (mLT-HSCs) that is prevalent among aged LT-HSCs. We identify CD61 as a marker of mLT-HSCs, and show that CD61-high LT-HSCs are uniquely primed to respond to acute inflammatory challenge. We predict several transcription factors to regulate mLT-HSCs gene program, and show that *Klf5*, *Ikzf1* and *Stat3* play an important role in age-related inflammatory myeloid bias. We have therefore identified and isolated a LT-HSC subset that regulates myeloid versus lymphoid balance under inflammatory challenge and with age.

One sentence summary

*Correspondence: mati@calech.edu. **Correspondence: aregev@broadinstitute.org. ***Correspondence: baltimo@caltech.edu.

Author Contributions

M.M., A.M., and D.B. designed the study with assistance from C.G.D and M.S.K. M.M., conducted experimental work with assistance from A.M., K.L., and P.H. M.S.K, N.R, A.R.K, D.F, M.M, A.M, P.H, K.L conducted bulk and single cell RNA sequencing and sample perpetrations. C.G.D performed bioinformatics analysis. M.M., A.M, A.R, and D.B. wrote the manuscript with contributions from C.G.D and M.S.K.

Declaration of Interests

The authors declare no competing interests.

Data and software availability

The accession number for the sequencing data in this paper is GEO: GSE100428.

Hematopoietic stem cells display transcriptional and phenotypic heterogeneity that is quantitatively altered with age and leads to the age-dependent myeloid bias evident after inflammatory challenge.

Keywords

Hematopoietic stem cells; stem cell aging; inflammation; single-cell RNA-sequencing

Introduction

Long-term hematopoietic stem cells (LT-HSCs) encounter continued stresses throughout life, yet maintain appropriate immune cell output (Akunuru and Geiger, 2016; Denkinger et al., 2015; Dykstra et al., 2011; Geiger et al., 2013; Morita et al., 2010; Sawai et al., 2016; Yamamoto et al., 2018). These stresses include replicative stress (Bernitz et al., 2016; Flach et al., 2014; Wang et al., 2012), as well as acute and chronic infectious challenge (King and Goodell, 2011; Nagai et al., 2006). Physiologic aging in both humans and mice leads to permanent changes in LT-HSC function, such as myeloid-biased hematopoietic output, and poor response to infections (Akunuru and Geiger 2016). This is often accelerated in settings of chronic inflammation and, when dysregulated, can lead to replicative exhaustion and extramedullary hematopoiesis (Esplin et al., 2011; Mehta et al., 2015).

Hematopoietic stem and progenitor cells (HSPCs) express innate immune receptors (King and Goodell, 2011), such as toll-like receptors (TLRs), and respond to many inflammatory mediators, including IFN-γ (Baldridge et al., 2010), M-CSF (Mossadegh-Keller et al., 2013), and the gram-negative bacterial component lipopolysaccharide (LPS) (Nagai et al., 2006). In response to acute LPS exposure, LT-HSCs increase proliferation, mobilize to the peripheral bloodstream (King and Goodell, 2011), and initiate emergency myelopoiesis to increase the system's output of innate immune cells (Haas et al., 2015). This increased output may also be mediated by hematopoietic progenitors, such as multipotent progenitors (MPPs) (Pietras et al., 2015; Young et al., 2016), in part due to direct secretion of cytokines that drive myeloid differentiation (Zhao et al., 2014).

Several hypotheses have been proposed to explain the age related changes in LT-HSC function (Kovtonyuk et al., 2016). First, cell-intrinsic changes within each aged LT-HSC might make it inherently myeloid-biased (Grover et al., 2016; Rossi et al., 2005). Second, the LT-HSC population may be comprised of subsets of myeloid- and lymphoid-biased cells, the composition of which changes with age such that myeloid-biased LT-HSCs are more prevalent within the aged LT-HSC population (Dykstra et al., 2007; Gekas and Graf, 2013; Yamamoto et al., 2013). The true nature of these age-related changes may in fact be a combination of both of these hypotheses, such that with age there is a growing subset of more intrinsically myeloid-biased LT-HSCs.

The transcriptional and functional state of LT-HSCs in steady state and in response to inflammatory mediators may help shed light on these questions, but is currently still poorly understood. A number of epigenomic and transcriptomic changes have been observed during bulk and single-cell expression analysis of young and aged LT-HSCs (Cabezas-Wallscheid et

al., 2014; Grover et al., 2016; Kowalczyk et al., 2015; Sanjuan-Pla et al., 2013; Sun et al., 2014; Yu et al., 2016). However, it is unclear if and how these changes lead to altered LT-HSC function, as seen with age-related myeloid bias (Dykstra et al., 2011; Gekas and Graf, 2013; Yamamoto et al., 2018). In particular, a previous study using single-cell RNA-seq (scRNA-seq) (Kowalczyk et al., 2015) of steady-state, resting LT-HSCs has not identified a subpopulation structure. An understanding of how inflammatory mediators effect LT-HSCs response and how this response changes with age may therefore help elucidate the underlying mechanism of age-related myeloid bias. This may further provide insight into age-related pathologies, such as improper immune responses to vaccines or infectious challenge, and the development of myeloid leukemia.

In this work, we investigate the acute inflammatory response of mouse HSPCs *in vitro* and *in vivo*, and how this response may be altered with age (Figure 1A). We show that major HSPC subtypes respond transcriptionally to inflammatory stimuli and that age-dependent inflammatory myeloid bias is intrinsic to LT-HSCs, based on bone marrow transplant experiments. Using scRNA-seq we find that the LT-HSC compartment is comprised of at least two subsets that become apparent upon stimulation. One of these subsets has features consistent with myeloid-bias (referred to as mLT-HSCs), with distinct cell-intrinsic responses to inflammatory stimulation. The myeloid-biased subset expresses high levels of the surface marker CD61, can be prospectively isolated and lead to myeloid bias upon reconstitution, and increases dramatically with age. We further identify putative transcriptional regulators of mLT-HSCs, and demonstrate the role of these regulators in age-related myeloid bias and differential responses to TLR ligands.

Results

Inflammation in aged and young mice leads to differential increases in myeloid output

To investigate the acute inflammatory response of hematopoietic progenitors from mice at different ages, we challenged 8–12 week old (‘young’) and 20–24 month old (‘aged’) mice with a single intraperitoneal injection of LPS (0.5mg/kg, Figure S1A-D). We observed a greater than twofold increase in peripheral blood myeloid frequencies in aged mice by 72 hours post-challenge, whereas only a minimal increase was seen in young mice (Figure S1A,B). These changes in myeloid output returned to baseline frequencies by 9 weeks post-challenge. The baseline frequency of T cells in aged mice was twofold lower than in young mice but both cohorts had increased T cell output 72 hours after LPS challenge (Figure S1C). In contrast, B cell output in both young and aged cohorts were decreased after LPS treatment, and the acute response was particularly dramatic in aged mice, which had a twofold loss in the frequency of B cells by 72 hours, and then recovered to baseline levels by 6 weeks post-challenge (Figure S1D). Aged mice therefore demonstrated a strong acute increase in myeloid output in response to inflammatory challenge that was not observed in young mice.

To evaluate the cumulative effect of acute inflammatory challenges on myeloid output, we performed a second LPS injection to all cohorts 1 month after the initial challenge. This resulted in an upregulation of peripheral blood myeloid cells in aged mice whereas again, only a milder increase in myeloid output was seen in young mice (Figure 1B,C).

Interestingly, while myeloid output in young mice returned to baseline within 3 weeks, aged mice myeloid cell frequencies mildly decreased 3 weeks post injection, but remained higher than baseline for at least 9 weeks post injection (Figure 1B,C). T cell levels slightly increased in young mice by 72 hours and did not change in aged mice (Figure 1D). Conversely, B cell output decreased in both aged and young mice by 72 hours, but while young B cells returned to baseline levels, aged mice B cell levels remained lower than baseline by 9 weeks post injection (Figure 1E).

The spleens of stimulated aged mice revealed increased myeloid cell frequencies and a dramatic loss of T cells compared to young mice (Figure S1E). Finally, bone marrow of stimulated aged mice had a three-fold enrichment for LT-HSCs compared to stimulated young mice, with a milder enrichment in short-term HSCs (ST-HSCs) and MPPs (Figure S1F). This enrichment in LT-HSCs is higher than the two-fold enrichment reported between unstimulated aged and young mice (Beerman et al., 2010; Mehta et al., 2015). These results suggest that repeated acute inflammatory stimuli in aged mice enhance myeloid-biased output from HSPCs and that the differences in immune cell output might originate from LT-HSCs.

Inflammation leads to a distinctive, long-term myeloid-biased output in aged LT-HSCs

To examine whether inflammation leads to a cell-intrinsic myeloid bias in LT-HSCs, we tested the impact of stimulation on the ability of young and aged LT-HSCs to reconstitute the immune system. Specifically, we first sorted LT-HSCs, ST-HSCs and MPPs from young and aged CD45.2 C57BL/6 mice. The sorted cells were either maintained unstimulated or stimulated with LPS and Pam3csk4 for 2 hours *in vitro*, and subsequently transplanted into lethally irradiated young CD45.1 C57BL/6 mice. Peripheral blood counts of CD45.2 expressing cells were monitored for four months (Figure 1F-I and Figure S2A,B). Both unstimulated and stimulated, young and aged LT-HSCs demonstrated long-term reconstitution of the immune system in primary, as well as secondary transplanted mice (Figure S2A-D).

At 3 months post-reconstitution (*i.e.*3 months after the *in vitro* LPS and Pam3csk4 challenge), inflammatory challenge of young LT-HSCs did not lead to altered peripheral blood myeloid and lymphoid cell frequencies compared to unstimulated controls (Figure 1F-I). As previously reported (Beerman et al., 2010; Pang et al., 2011), unstimulated aged LT-HSCs had higher peripheral blood myeloid output and lower lymphoid output compared to unstimulated young LT-HSCs (Figure 1F-I). However, stimulated aged LT-HSCs demonstrated a marked additional increase in the frequency of peripheral blood myeloid cells (Figure 1F,G) and a further decrease in the frequency of peripheral blood B cells (Figure 1H). Thus, aged LT-HSCs demonstrated myeloid-biased ‘memory’ of the initial *in vitro* LPS and Pam3csk4 challenge that persisted for several months post-reconstitution, a phenomenon not seen with stimulated young LT-HSCs. Interestingly, no significant difference in LT-HSC frequency was observed between cohorts, including in the previously identified myeloid-biased $CD41^{+}$ LT-HSC subpopulation (Gekas and Graf, 2013) (Figure S2E-H). These results suggest that direct TLR stimulation of aged LT-HSCs leads to a long-

term increase in myeloid bias. It is not clear, however, whether this increase is cell intrinsic or due to changes in composition of LT-HSCs population.

HSPCs demonstrate a canonical transcriptional response to TLR ligands

We hypothesized that the differential effects of young and aged stimulated LT-HSCs may be due to a variable transcriptional response to inflammatory signals. To test this hypothesis, we measured the transcriptional profiles of populations of HSPCs from young and aged mice during a 12-hour time-course of LPS and Pam3csk4 stimulation *in vitro* (Figure 2A). LT-HSCs, ST-HSCs and MPPs from both young and aged mice all demonstrated a robust and similar transcriptional response to inflammatory stimuli (Figure 2B and Table S1), which largely resembled that seen in mature cell types with different physiological functions, such as bone marrow derived dendritic cells (BMDCs) after LPS stimulation (Figure 2B-D) (Jovanovic et al., 2015). This includes the same temporal ordering of induction in inflammatory gene clusters as in mature cell types (Amit et al., 2009; Ramirez-Carrozzi et al., 2009), up-regulation of NF-κB-related genes (Figure 2C) (Bhatt et al., 2012; Hao and Baltimore, 2009), and induction of the expression of several effector cytokines (Figure 2D), albeit at slightly lower levels (Figure S3A-C). Among the differentially expressed genes between all cell types, HSPCs from both young and aged mice presented similar patterns compared to BMDCs (Figure 2B; for a complete list of differentially expressed genes and their Gene Ontology (GO) enrichments see Table S2). Thus, the response of young and aged HSPCs to inflammatory activation resembles the canonical response of mature cells to similar stimulation, both in the identity of the regulated genes and in the timescale of the response. This suggests that the differences in the reconstitution outcome were not simply related to differences in the transcriptional response when measured at the population level.

Single-cell RNA-seq reveals two subsets of LT-HSCs with distinct responses to inflammatory stimulus

Next, we considered the possibility that there are different subsets of LT-HSCs either in steady state or post-stimulation (“cell intrinsic changes”), and that their relative proportions may change with age (“compositional changes”). Early hematopoietic progenitors are comprised of heterogeneous functional subpopulations (Benz et al., 2012; Gekas and Graf, 2013; Morita et al., 2010; Sanjuan-Pla et al., 2013), which often reveal themselves in response to inflammatory stimuli (Haas et al., 2015; Zhao et al., 2014). While a previous scRNA-seq study we performed of LT-HSCs has mostly revealed age-related differences in the cell cycle (Kowalczyk et al., 2015), we hypothesized that stimulation could unveil additional cell intrinsic distinctions that were not observed in resting cells.

To determine the composition of HSPCs in each age group and condition, we performed full-length scRNA-seq (Picelli et al., 2013) of young and aged LT-HSCs, ST-HSCs and MPPs, with and without 2 hours of *in vitro* LPS and Pam3csk4 stimulation of sorted cells. As we aimed to distinguish cell intrinsic, possibly subtle, stimulus-specific states within a very well-defined cell population, we opted for the deeper-coverage full length scRNA-Seq approach over massively parallel approaches (Tanay and Regev, 2017; Wagner et al., 2016). We profiled 2,046 individual cells from nine mice (5 young, 4 aged), with 124–186 cells for each given cell type and condition. In order to eliminate sources of variability resulting from

known confounding factors, we removed 611 cells as low-quality and 58 as possible contaminants (STAR-Methods). In addition, 578 of the cells were actively cycling (STAR-Methods). Overall, we retained 949 cells for subsequent analysis, comprised of 187 MPPs, 404 ST-HSCs, and 358 LT-HSCs.

We identified three major groups of cells using unsupervised clustering (STAR-Methods), denoted clusters 1, 2 and 3 (Figure 3A). Cluster 1 (311 cells) contained most (302 of 354) of the unstimulated HSPCs of all types, forming a continuum from MPPs to LT-HSCs (Figure 3B), with aged and young LT-HSCs clustering together (Figure 3D), and hardly any stimulated cells. Clusters 2 (103 cells) and 3 (421 cells) almost exclusively contained stimulated HSPCs (Figure 3C), and had opposing patterns with respect to aged and young LT-HSCs (Figure 3E): cluster 3 contained 77% of the aged stimulated LT-HSCs and only 13% of the young stimulated LT-HSCs, whereas cluster 2 had 72% of the young stimulated LT-HSCs, and only 10% of the aged stimulated LT-HSCs (Figure 3E). This suggests that there are distinct subsets of LT-HSCs in the bone marrow that can be discerned by their different cell intrinsic responses to stimulation, and that the relative frequencies of these subsets appear to change with age. Of note, the distinction between these LT-HSC subsets could only be discerned with stimulation, and no significant difference was found within unstimulated or stimulated ST-HSCs or MPPs (Figure S3D,E). Given these findings, we focused further analysis on LT-HSCs.

Myeloid-biased LT-HSCs can be identified by a distinct gene signature under inflammatory conditions

To identify the differences between stimulated LT-HSCs in cluster 3 and cluster 2, we examined genes that were differentially expressed between the two clusters. Cluster 3-specific genes were enriched for genes related to myeloid function and inhibiting lymphoid differentiation, including pathways related to NF-κB localization, negative regulation of lymphocyte development, macrophage proliferation, cell migration and localization, and platelet derived growth factor signaling (Figure S3F). Cluster 2-specific genes were enriched for genes involved in lymphocyte development, cell proliferation, and the acute inflammatory response (Figure S3G). Cells in any given cluster, regardless of age, were similar to each other and distinctly different from cells in the other cluster. These data are consistent with a model where aged and young LT-HSCs have different proportions of cells that display unique lineage-biased pathway preferences in response to inflammatory signals.

To test whether the LT-HSC subsets also exist in unstimulated cells in steady-state conditions, we identified 47 genes that were significantly differentially expressed both when comparing cluster 3 *vs.*cluster 2 (single cell differential expression, 'SCDE' (Kharchenko et al., 2014), FDR < 0.01) and when comparing unstimulated aged *vs.* young LT-HSCs within cluster 1 (Figure S3H; STAR-Methods, SCDE FDR < 0.1). We then tested whether these 47 genes coherently co-vary across the 149 unstimulated LT-HSCs, and thus might reflect a variable cell state within these cells. Indeed, we identified three distinct co-varying gene clusters (Figure 3F), two of which contained genes involved in myeloid and platelet differentiation, including *Selp*, *Vwf*, *Gpr64*, *Plscr2*, and *Wdfy1*. Notably, recent studies have reported myeloid-biased CD41, Vwf or CD150-high expressing LT-HSC subpopulations

(Dykstra et al., 2011; Gekas and Graf, 2013; Sanjuan-Pla et al., 2013); in our analysis, aged LT-HSCs have increased yet variable expression of CD150 and Vwf, and no significant difference in CD41 expression (Figure S3I-K).

Next, we generated a refined gene signature. We first scored unstimulated LT-HSCs with the initial set of 47 genes (Figure S3H), identifying two putative cell subsets (STAR Methods). Next, we used these subsets to initialize *k*-means clustering (k=2) within the unstimulated LT-HSCs. We used the identities of the cells based on this clustering to designate them as myeloid-biased LT-HSCs (mLT-HSCs), and non-myeloid biased LT-HSCs (nmLT-HSCs).We tested these two final clusters for differentially expressed genes, finding 365 upregulated genes and 34 downregulated genes in the mLT-HSC cluster, which we use to define our "mLT-HSC signature" (SCDE FDR < 0.1 and the same direction of change as for stimulated mLT-HSCs) (Table S3).

In the final *k*-means clusters, 92% of cells in the myeloid biased cluster were aged cells and only 8% were young cells (Figure 3G, to the right of the dashed line), while only 20% of cells in the non-myeloid biased cluster were aged cells and 80% were young cells (Figure 3G, to the left of the dashed line). This is consistent with our findings that the frequency of stimulated mLT-HSCs increases with age (Figure 3E). Applying the same signature to our stimulated LT-HSCs or to an independent dataset of unstimulated aged and young LT-HSCs from two mouse strains (Kowalczyk et al., 2015) showed consistent results: while the LT-HSC population is inherently heterogeneous, more aged LT-HSCs score highly for the mLT-HSC signature (Figure S3L,M). Thus, the mLT-HSC signature allowed us to identify the subtle portion of myeloid-biased like cells among the young unstimulated LT-HSCs, and to show that the proportion of high-scoring mLT-HSC cells rises with age.

Klf5, Ikzf1 and Stat3 regulate age-related inflammatory myeloid bias of LT-HSCs

To identify transcription factors (TFs) that may regulate differentially expressed genes between the mLT-HSC and nmLT-HSC subsets, we looked for enriched TF motifs in the enhancer sequences associated with these genes (Lara-Astiaso et al., 2014) (Figure 3H). In particular, we focused on TFs that themselves were differentially expressed between mLT-HSCs and nmLT-HSCs, since altered transcriptional regulation of a TF may affect its target genes. Among the nine significant TFs whose motifs were enriched in enhancers of differentially expressed genes were *HoxA9*, *Klf4*, *Klf5*, *Ikzf1*, and *Stat3*, which we chose to further test given their known putative roles in HSPC biology (Figure 3H; blue dots).

To test the role of these TFs in age-related myeloid bias, we transplanted young or aged HSPCs with shRNA knockdowns of each TF into young irradiated C57BL/6 recipient mice (Figure S4A). Of the tested TFs in steady state, *Klf5, Ikzf1, and Stat3* had significant, age-dependent effects, whereas *HoxA9* and *Klf4* did not (Figure S4B-E). Consistent with the upregulated expression of *Klf5* in mLT-HSCs, we found that knockdown of *Klf5* in aged LT-HSCs resulted in increased lymphoid output (Figure S4C) and decreased myeloid output to levels seen with control young LT-HSCs (Figure S4D,E). There was no immediately apparent effect of *Klf5* knockdown in young LT-HSCs. Knockdown of *Ikzf1* in young LT-HSCs resulted in decreased lymphoid output (Figure S4C). Interestingly, loss of *Ikzf1* in aged LT-HSCs had no significant effect on lymphoid output, but like knockdown of *Klf5*, it

resulted in decreased myeloid output to levels seen with control young LT-HSCs (Figure S4D,E).

We next tested whether these TFs regulate myeloid output of LT-HSCs under conditions of inflammatory stress. To do this, we challenged the aforementioned shRNA knockdown mice with LPS (as in Figure 1B-E). As expected, after the LPS challenge, mice transplanted with control aged LT-HSCs showed a sustained upregulation of myeloid output over the 3 weeks (Figure 4A-C, solid red lines), whereas mice transplanted with control young HSPCs had only a transient increase in myeloid output followed by rapid recovery to baseline (Figure 4A-C, solid black lines). The response to LPS of mice transplanted with aged HSPCs expressing *Klf5, Ikzf1* or *Stat3* shRNAs phenocopied that of mice transplanted with control young HSPCs (Figure 4A-C and Figure S4F-H, dashed red lines). Thus, *Klf5*, *Ikzf1*and *Stat3* may play a critical role in regulating inflammatory myeloid bias in aged LT-HSCs. No dysregulation in immune output was seen in mice transplanted with HSPCs expressing *HoxA9*, *Klf4* or *Zbtb4* shRNAs (data not shown).

To identify the cell types responsible for the changes observed after *Ikzf1*, *Stat3* or *Klf5* knockdown in aged HSPCs, we analyzed the bone marrow compartment of all mice 3 months post-transplantation. Mice transplanted with aged control cells had higher LT-HSC and CMP frequencies, and lower CLP frequencies, but no changes in other early progenitor populations when compared to mice reconstituted with young control cells (Figure 4D-F and Figure S4I-K). Knockdown of either *Klf5*, *Ikzf1* or *Stat3* in transplanted aged HSPCs resulted in a decreased frequency of LT-HSCs compared to control aged HSPCs (Figure 4D). We observed no significant effect on the frequency of LT-HSC in the bone marrow in mice transplanted with young HSPCs expressing any of these knockdown constructs (Figure 4D, grey bars) or in aged HSPC transplanted mice expressing *HoxA9* or *Klf4* shRNAs (data not shown). These data therefore suggest that *Klf5*, *Ikzf1* and *Stat3* may regulate inflammatory myeloid bias in aged LT-HSCs and may do so by altering the function and frequency of LT-HSCs in the bone marrow compartment.

To investigate if the expression of *Ikzf1, Stat3* and *Klf5* is sufficient to skew the LT-HSC output, we over-expressed these genes in young and aged HSPCs, and transplanted these cells into young irradiated C57BL/6 mice (STAR Methods). *Ikzf1* and *Klf5* overexpression (OE) led to an increase in myeloid output and decrease in lymphoid output at 3 months post-reconstitution with both young and aged HSPC donor cells (Figure 4G-I and Figure S5A-C). A significant increase in myeloid output was observed after a single LPS injection in *Ikzf1* and *Klf5* OE mice compared to age appropriate controls. Conversely, *Stat3* OE in both young and aged donor HSPCs yielded comparable myeloid output, which resembled that of aged control mice following LPS injection (Figure 4G-I and Figure S5A-C, dashed lines). Analysis of the bone marrow compartment of *Klf5* OE mice revealed a marked increase in the frequency of LT-HSCs, but no differences in frequency of ST-HSCs or MPPs. *Klf5* OE did affect downstream progenitors, yielding a higher frequency of bone marrow CMPs and GMPs, and a decrease in frequency of CLPs in both young and aged donors compared to age-matched controls (Figure 4J-L and Figure S5D-H). Similarly, *Ikzf1* OE in both young and aged mice resulted in an increase in bone marrow LT-HSC frequency and decrease CLP and LMPP frequencies. *Stat3* OE did not significantly alter LT-HSC frequencies in young or

aged mice (Figure 4J-L and Figure S5D-H). This data therefore suggests that *Klf5, Ikzf1*and *Stat3* may be necessary and sufficient to promote inflammatory myeloid bias.

CD61 is a marker for mLT-HSCs

To identify putative surface markers that may characterize mLT-HSCs, we searched the set of genes that were differentially expressed between mLT-HSCs and nmLT-HSCs for those encoding surface proteins that also have a commercially available antibody (Figure S6A and Table S4). Among the surface proteins whose gene expression was elevated in mLT-HSCs compared to nmLT-HSCs were CD61 (Itgb3), CD62p, CD166, CD38 and CD34 (Figure S6A). We tested the surface expression of five of these proteins in aged and young LT-HSCs using flow cytometry (Figure 5A and S6B), and identified CD61 as the most differentially expressed surface protein between the two populations (Figure 5A). The relative proportion of high CD61 expressing LT-HSCs (CD61-high LT-HSCs) and low CD61 expressing LT-HSCs (CD61-low LT-HSCs) was consistent with the proportions of mLT-HSCs and nmLT-HSCs, respectively, as identified in aged and young mice (Figure S6C, D). CD61 encodes for β3 integrin. In hematopoietic cells, CD61 has been shown to heterodimerize with α_V/CD51, α_5/CD49e, and α_{IIB}/CD41 to form $\alpha_V\beta_3$, $\alpha_5\beta_3$, or the platelet specific $\alpha_{IIB}\beta_3$integrins, respectively (Nemeth et al., 2007; Shattil et al., 1998). Using flow cytometry, we found that on LT-HSCs CD51 expression levels correlates most to that of CD61, while CD49e and CD41 expression was only partially correlated with CD61 (Figure S6E-G, Figure S2F,H).

We next tested if CD61-high LT-HSCs are functionally myeloid biased. We sorted CD45.2 CD61-high and CD61-low LT-HSCs (Figure S6C,D) from both young and aged mice, and transplanted them into young lethally irradiated CD45.1 C57BL/6 mice. At three months post-reconstitution, the peripheral blood from mice transplanted with either young or aged CD61-high LT-HSCs had decreased T cell and B cell output, and increased myeloid and granulocyte output (Figure S7A-D), compared to mice transplanted with young CD61-low cells. To test if CD61-high LT-HSCs are more prone to inflammatory myeloid bias, we challenged these transplanted mice with LPS. Mice transplanted with both young and aged CD61-high LT-HSCs had a more pronounced and sustained increase in peripheral blood myeloid and decrease in lymphoid output 3 weeks post-challenge when compared to mice transplanted with total LT-HSCs and CD61-low LT-HSCs of comparable age (Figure 5B-E and Figure S7E-H).

To investigate the cellular basis of myeloid bias with transplant of CD61-high LT-HSCs, we harvested bone marrow from all transplanted mice and analyzed for early hematopoietic progenitors. The bone marrow of mice that had received CD61-high LT-HSCs, whether young or aged, had increased frequencies of LT-HSCs (Figure 5F) of which the majority were CD61-high LT-HSCs compared to mice transplanted with CD61-low LT-HSCs (Figure 5G; 56% and 74% of total LT-HSCs in mice transplanted with young and aged CD61-high LT-HSCs, respectively). The frequency of CD61-high LT-HSCs in mice transplanted with either young or aged CD61-low LT-HSCs were similar to that of mice transplanted with total LT-HSCs of young mice, and over three-fold lower than that of mice transplanted with CD61-high LT-HSCs or total aged LT-HSC mice (Figure 5G). This suggests there CD61-low

LT-HSCs may have the potential to convert to a CD61-high LT-HSC phenotype. Consistent with their myeloid-biased phenotype, mice transplanted with CD61-high LT-HSCs had decreased bone marrow CLPs (Figure 5H), and increased GMPs, CMPs and MEPs (Figure 5I-K) compared to mice transplanted with CD61-low LT-HSCs, regardless of age.

Discussion

In this work, we demonstrate that LT-HSCs have a heterogeneous response to inflammatory stimuli that is altered with age. We show that even the most multipotent of HSPCs directly respond *in vitro* to TLR ligands with a potent transcriptional response. Using scRNA-seq, we demonstrate that both the young and aged LT-HSC compartments are comprised of at least two distinct subsets of cells with a defined molecular signature. We identify CD61 as a marker of inflammation-responsive myeloid-biased LT-HSCs (mLT-HSCs). We posit that an increased proportion of mLT-HSCs in the bone marrow is a key driver of myelopoiesis and further identify several transcription factors that regulate steady state and inflammatory myeloid bias in aged LT-HSCs. Together, our data suggests a revised model (Figure 6) of how inflammation impacts LT-HSC function and composition with age.

We show that various types of HPSCs respond transcriptionally to TLR ligands *in vitro* in a similar way to that seen in BMDCs after LPS stimulation (Ramirez-Carrozzi et al., 2009). Given the different functional roles of HSPCs and mature immune cells, this similarity in transcriptional response is surprising. It has been suggested that, as in mature cell types, inducing the expression of NF-κB with LPS and Pam3csk4 in HSPCs may affect cytokine secretion and proliferation (Zhao et al., 2011, 2014). We observed that the dynamics of expression of NF-κB-driven genes was largely similar between HSPCs and BMDCs. Thus, the majority of NF-κB-responsive genes appear to be regulated similarly in both HSPCs and mature cells.

While it has been demonstrated that TLR stimulation of LT-HSCs induces their proliferation (Zhao et al., 2013), our results suggest that it does not alter their long-term reconstitution potential. Importantly, aged LT-HSCs maintained a memory of the *in vitro* inflammatory challenge and had increased myeloid output 3 months after transplant compared to unstimulated aged LT-HSCs. These data therefore confirm that LT-HSCs directly sense TLR ligands (Nagai et al., 2006), and in response to this, the aged LT-HSC population has an amplified cell-intrinsic myeloid bias. In the context of physiologic aging, it might be that the accumulation of inflammatory challenges over the lifetime of an animal results in selection and expansion of mLT-HSCs, partially due to direct sensing of these inflammatory signals by these cells. mLT-HSCs enrichment, in turn leads to myeloid bias, further amplifying chronic inflammation, forming a positive feedback loop generating mLT-HSCs expansion. This hypothesis is supported by the fact that chronic inflammatory stimulation of young mice, either by repeated LPS challenge or another form of NF-κB activation, leads to myeloid-biased output (Esplin et al., 2011; Zhao et al., 2013). Additionally, human chronic inflammatory diseases such as rheumatoid arthritis in relatively young individuals present with functional changes in HSPCs and a myeloid bias, mirroring aged individuals (Wunder and Henon 2012; Colmegna et al. 2008). Given that the LT-HSC population is heterogeneous, it is yet to be determined whether inflammation plays a role in either

expanding the number of cells in the mLT-HSC state or in changing the state of nmLT-HSCs to an mLT-HSC-like state over time.

Using scRNA-seq, we identified subsets within the LT-HSCs population, with distinct transcriptional responses to inflammatory signals. Previous efforts have identified phenotypic markers for megakaryocyte and myeloid biased LT-HSC subpopulations (Dykstra et al., 2011; Gekas and Graf, 2013). The gene signature in this study provides functional insight into the basis of myeloid bias in the context of aging and inflammation. Using this gene signature from stimulated LT-HSCs, we uncovered a subset of mLT-HSC-like cells enriched in the unstimulated aged LT-HSC compartment that have the potential to respond uniquely to acute inflammatory signals. This is consistent with recent results suggesting that there is an epigenetically primed subset of LT-HSCs that is uniquely poised to respond to LPS (Yu et al., 2016). We show herein that such a subset may also be identified using mRNA expression data.

We identified CD61 as a functional surface marker for mLT-HSCs. CD61-high LT-HSCs from both young and aged mice led to myeloid bias in transplantation experiments, confirming it as a phenotypic marker for mLT-HSCs. CD61 is the b3 integrin subunit, which dimerizse with ItgaV (CD51) to form the vitronectin receptor Itgb3aV predominantly expressed on macrophages, osteoclasts, dendritic cells and platelets. CD61 expression has been shown to contribute to LT-HSC repopulating efficiency (Umemoto et al., 2008), quiescence (Umemoto et al., 2006), and proliferation (Khurana et al., 2016). Consistent with this, we see that reconstitution efficiency in CD61-low LT-HSCs from both young and aged mice is hampered compared to CD61-high and total LT-HSCs (Figure S7I). Interestingly, our transplantation experiments with purified CD61-low and CD61-high LT-HSCs resulted in a distribution of CD61 expression in LT-HSCs resembling young and aged total LT-HSC transplants, respectively. This suggests that there may be plasticity between mLT-HSC and nmLT-HSC subpopulations, and supports the hypothesis that the composition of intrinsically myeloid biased LT-HSCs changes with age. While we show CD61 can be used as a phenotypic marker, whether it has a functional role in the formation of mLT-HSCs is yet to be determined.

We additionally identified several transcriptional regulators of inflammatory myelopoiesis in aged stimulated mLT-HSCs. Among these was *Klf5*, which is required for embryonic stem cell self-renewal (Jiang et al., 2008). The enrichment of *Klf5* in mLT-HSCs may therefore play a role in the increased symmetric self-renewal divisions seen in aged LT-HSCs (Geiger et al., 2013; Sudo et al., 2000). Indeed, knockdown of *Klf5*in aged LT-HSCs, but not in young LT-HSCs, results in decreased myeloid output and decreased LT-HSC bone marrow frequency, while overexpression leads to the opposite effect. Consistent with these results, it has recently been shown that deficiency of *Klf5* in LT-HSCs leads to decreased bone marrow homing of these cells in transplant experiments and reduced output of myeloid cells, especially neutrophils (Shahrin et al., 2016; Taniguchi Ishikawa et al., 2013).

The role of *Ikzf1* in LT-HSC function is less well understood. Previous studies have suggested that *Ikzf1* does not play a role in myeloid versus lymphoid lineage commitment of young LT-HSCs (Ng et al., 2009). Our results suggest that in the context of inflammation,

Ikzf1 may indeed have a positive role in myeloid fate decisions. We found that any perturbation of *Ikzf1* expression levels affects the differentiation potential of LT-HSCs. Consistent with this, *Ikzf1* has been shown to bind enhancer elements of both myeloid and lymphoid genes in human HSPCs (Novershtern et al., 2011). Knockdown of *Stat3* in aged LT-HSCs also severely hampered myeloid output after inflammatory challenge. This is consistent with the role of *Stat3* as a major inflammatory TF. In particular, some studies suggest that *Stat3* is induced in response to TLR4 signaling in certain cell types (Kortylewski et al., 2009). Interestingly, complete knockout of *Stat3* in LT-HSCs has been shown to result in a premature aging phenotype (Mantel et al., 2012); our results suggest that partial loss of *Stat3* is not enough to recapitulate this phenotype.

In summary, our analysis has uncovered mLT-HSCs, identified CD61, a previously unreported marker for inflammation-responsive myeloid-biased LT-HSCs, and revealed three TFs, *Klf5*, *Ikzf1*, and *Stat3* as important regulators of inflammatory myeloid bias. Since altering the expression of these TFs can alter the balance of myeloid and lymphoid cells during emergency myelopoiesis, manipulating them or other aspects of the unstimulated or stimulated mLT-HSC programs may provide new therapeutic avenues for re-establishing appropriate lymphoid versus myeloid balance to improve immune function and prevent myeloid leukemias with age.

STAR Methods

Contact for reagent and resource sharing

Further information and requests for resources and reagents should be directed to and will be fulfilled by the Lead Contact - Mati Mann, mati@caltech.edu

Experimental model and subject details

Mice—The California Institute of Technology Institutional Animal Care and Use Committee approved all experiments. Young and aged C57BL/6 WT males and females mice were obtained from Charles Rivers Laboratories and housed in the Caltech Office of Laboratory Animal Resources (OLAR) facility. For all experiments, young mice were between 8–12 weeks of age and aged mice were between 20–24 months of age.

Method Details

Flow cytometry—Tissues were first harvested and cells were homogenized. Samples were depleted of RBCs using RBC lysis buffer (BioLegend). Cells were subsequently stained with fluorescently labeled antibody. Respective cell types were analyzed according to relevant surface markers by using the following antibodies: CD45.1 and CD45.2, lineage-specific markers (CD11b, Gr-1, CD19, B220, CD3e, Nk1.1 and Ter119), or progenitor-specific markers (CD150, CD48, Flt3, CD34, FcRgamma and IL7R). All antibodies were purchased from BioLegend. HSPCs were sorted by first lineage-depleting whole bone marrow from young and aged mice. Samples were incubated with biotin-conjugated lineage antibodies (CD19, B220, CD4, CD8, CD11b, Gr-1, Ter119, Nk1.1, IL7Ra each at 1:200 dilution), and passaged through Miltenyi MACS negative selection columns. Cells were subsequently analyzed with a MACSQuant10 Flow Cytometry machine (Miltenyi), or sorted using BD

Aria sorter. HSPCs were sorted using SLAM markers with the following gating strategies: for MPPs: Lineage-cKit+Sca1+CD150-CD48+, for ST-HSCs: Lineage-cKit+Sca1+CD150-CD48- and for LT-HSCs: Lineage-cKit+Sca1+CD150+CD48-, with or without CD61. Gating strategies for other cell types used in our analysis are described in Figure S8. (Complete list of antibodies catalog numbers and lots can be found in Key Resources table)

Cell culture—Cells were cultured in a sterile incubator that was maintained at 37^0C and 5% CO_2. Primary cells were cultured in HSPC media, comprised of complete RPMI supplemented with 10% FBS, 100 U/mL penicillin, 100 U/mL streptomycin, 50uM β-mercaptoethanol and mouse SCF (50 ng/mL), IL-3 (20 ng/mL), and IL-6 (50 ng/mL) when cultured for reconstitution experiments. 293T cells were cultured in DMEM supplemented with 10% fetal bovine serum, 100 U/mL penicillin and 100 U/mL streptomycin. For *in vitro* stimulation, sorted HSPCs were incubated in HSPC media with 100ng/ml LPS (SIGMA CAT: L2880–100MG), and 1ug/ml Pam3csk4 (Invivogen CAT: 41–11-60–10) for the indicated time points.

Bone marrow transplant experiments—Bone marrow reconstitution experiments were performed using aged and young unmanipulated cells or with the vectors noted below. Aged and young WT CD45.2 C57BL/6 mice were treated with 5-fluorouracil (10ug; Sigma) for 5 days to enrich for hematopoietic stem and progenitor cells (HSPCs) in the bone marrow. After 5 days, bone marrow cells were harvested, red blood cells (RBCs) were lysed with RBC lysis buffer (BioLegend), and cells were plated in HSPC media (see above). Cells were then cultured for 24 hours and spin-infected for 2 hours at 30^0C and 2500RPM with PCL-ecotropic pseudotyped gamma-retrovirus expressing the shRNA or cDNA of interest (see Key Resources table). Virus supernatant was then removed and replaced with HSPC media. A second round of spin infection was performed 24 hours later. 24hrs after the last infection, recipient mice were lethally irradiated (1000 rads) and 250,000 virus-infected HSPCs were retro-orbitally delivered to reconstitute the immune system.

Recipient mice were monitored for health and peripheral blood was analyzed for mature blood cell types every 4 weeks or at 4 hours after each LPS injection up till secondary transplant, or till the experimental endpoint 16 weeks post-reconstitution. At each endpoint, immune organs were harvested for further analysis. The number of mice for each experimental cohort is described in the figure legends.

For LT-HSC, ST-HSC or MPPs, from either young or aged CD45.2 mice, donor bone marrow was extracted and lineage depleted cells were sorted for each cell population (see sorting procedure above). Cells were then processed for transplant or stimulated with LPS and Pam3csk4 as described above for 2 hours prior to transplantation. A total of 1000 sorted cells were injected together with 100,000 supporting CD45.1 bone marrow cells from young donors into irradiated young CD45.1 recipient mice. For secondary transplant experiments, 250,000–500,000 cells from whole bone marrow of primary transplant mice were transplanted into irradiated young CD45.1 recipient mice. For CD61 reconstitution experiments, 100 CD61 high or CD61 low LT-HSCs from young or aged CD45.2 mice were injected into irradiated young CD45.1 mice together with 200,000 supporting total bone

marrow cells from young CD45.1 mice. Each experiment was repeated at least twice, and in many cases three times.

In vivo LPS challenge—Mice were injected intraperitoneally with a sublethal dose of LPS (0.5ug/gram, SIGMA CAT: L2880–100MG), and were bled before injections, and after 24hrs, 7days, 14days and 7 weeks. Blood samples were analyzed for CD11b, CD3e, CD19, and Gr1 expressing cells to asses mature immune cell populations. In some cases, a secondary injection of 0.5ug/gram LPS was conducted followed by immune cell repertoire in peripheral blood as with the first injection. For chronic LPS injections, mice were injected with 0.1ug/gram twice weekly for 12weeks. Mice were then harvested, blood samples were analyzed for CD11b, CD3e, CD19, and Gr1 expressing cells to asses mature immune cell populations, and bone marrow cells were analyzed for LT-HSC, ST-HSC, MPP as well as CD61 on LT-HSCs.

Bulk RNA-seq—For bulk RNA-seq, LT-HSCs, ST-HSCs and MPPs from aged and young mice were sorted as described above. Cells were then stimulated *in vitro* for 0.5, 1hr, 2hr, 4hr, 8hr, or 12hr with 100ng/ml LPS (SIGMA CAT: L2880–100MG), and 1ug/ml Pam3CSK4 (Invivogen CAT: 41–11-60–10). mRNA extraction was performed using the PrepEase RNA Spin Kit (usb®). RNA quality was assessed using RNA 6000 Pico Kit (Agilent). Full-length RNA-seq libraries were prepared as previously described (Kowalczyk et al., 2015) and paired-end sequenced (38bp x 2) on an Illumina HiSeq2500.

Single-cell RNA-seq—For full-length single-cell RNA-Seq, LT-HSCs, ST-HSCs and MPPs from aged and young mice were sorted as described above and stimulated *in vitro* for 2 hours in large volumes (2000–3000 cells in 10mL of media) to minimize secondary stimulation with secreted cytokines. Single cells were subsequently sorted into 96 well plates containing 5ul TCL Buffer (QIAGEN) with 1% 2-mercaptoethanol, centrifuged and frozen at −80°C. SMART-Seq2 protocol was carried out as previously described (Picelli et al., 2013) with minor modifications (MSK and AR, in preparation). cDNA was amplified with 20 cycles and tagmented with a quarter of the standard Illumina NexteraXT reaction volume. Single-cell libraries were pooled and paired-end sequenced (38bp x 2) on an Illumina Hiseq2500 or Nextseq500.

DNA constructs—For *in vivo* Ikzf1, Klf4, Klf5, Hoxa9, Zbtb4, Stat3 shRNA experiments, the mature shRNA sequence was synthesized in the microRNA-155 loop-and-arms format (O'Connell et al., 2010) and cloned into the MSCV-eGFP (MG). All shRNA sequences are provided in Reagents and Resources. For overexpression of *Ikzf1*, *Klf5*, and *Stat3*, the cDNA of each transcription factor was cloned into a PIG vector (Mayr and Bartel, 2009) (Addgene plasmid # 21654). All cDNA sequences cloned are provided in Table S5. Virus production is described below.

Virus production—To generate retrovirus for HSPC infection, 10^6 HEK293T cells were first plated in a 15cm plate. 24 hours later, cells were transfected with both the pCL-Eco vector and either the MG or PIG vector with the relevant shRNA or cDNA described above for gene delivery. For transfection, we used BioT (Bioland Scientific) as per the

manufacturer's protocol. 36 hours after transfection, virus was collected, filtered through a 45uM syringe filter, and used for infection of HSPCs.

Quantification and statistical analysis

Bulk RNA-seq analysis—RNA-seq reads for both single cell and bulk were aligned to the mm9 UCSC transcriptome and quantified using RSEM (Bowtie versions 1.27 and 0.12.7, respectively) (Li and Dewey, 2011). Gene-level counts were TMM-normalized and edgeR (Robinson et al., 2010) was used to call differentially expressed genes, comparing each time point to time 0, for all cell types and mouse ages. We also considered baseline differences between cell types and mouse ages. P-values were adjusted for multiple hypothesis testing by Benjamini-Hochberg FDR correction, with FDR < 0.01 considered for subsequent analysis.

Single cell RNA-seq analysis—Cells that had fewer than 2000 genes detected, a lower than 25% rate of reads mapping to the transcriptome, or were undergoing the cell cycle (Kowalczyk et al., 2015) were excluded from analysis. We also excluded outlier cells from the MPPs group which were likely caused by cell contamination. To correct for batch issues, the two experimental batches were centered to have the same mean log(TP100K+1) (hereafter referred to as log(TPM), where TPM stands for 'transcripts per million') per gene. PCA was done in R with scaled, centered log(TPM), using only genes annotated with GO terms we considered important in our system, including cytokine receptor binding, immune system development, immune system process, inflammatory response, response to cytokine, single-organism developmental process, stem cell, cell proliferation, and autophagy. The permutationPA function from jackstraw (Chung and Storey, 2015) was used to select significant PCs and then tSNE (tSNE package, with default parameters) was used to reduce the data to two dimensions. Density-based clustering was performed (package dbscan, eps =5, minPts=20) and the resulting three clusters were used for subsequent analysis.

Single-cell differential expression and gene signatures—All single-cell differential expression analysis was performed with single cell differential expression (SCDE) (Kharchenko et al., 2014), considering only genes that had at least 50 reads and were detected in at least 5 cells. For all signatures, a cell's signature score is the weighted sum of log(TPM) of genes, weighted by the direction of the enrichment (either +1 for enriched genes or −1 for depleted genes).

Stimulated myeloid-biased LT-HSC signature.—Genes with a DE FDR <0.1 when comparing stimulated LT-HSCs in cluster 3 to cluster 2 were defined as the signature of stimulated myeloid-biased LT-HSCs.

Unstimulated myeloid-biased LT-HSC signature.—Genes where bulk RNA-seq data indicated a significant difference (FDR<0.01) in expression between both aged *vs.* young unstimulated LT-HSCs, and between cluster 3 *vs.* cluster 2 LT-HSCs (in the same direction) were used as an initial estimate of a *common* myeloid-biased LT-HSC signature. Next, a weighted sum of the genes in this common signature was used to score each of the unstimulated LT-HSCs, and the cells were partitioned into two groups on this basis. The

centroids of these two groups of cells were used to initialize *k*-means clustering (*k*=2) of the unstimulated LT-HSCs, performed in PC-space with PCs 2–10 of a PCA of all expressed genes in unstimulated LT-HSCs only (PC1 was correlated with batch, and so was excluded here). This yielded two new clusters, similar but distinct from those with which we initialized the k-means clustering algorithm. SCDE was used to identify differentially expressed genes (FDR<0.1) between the cells in these two clusters (representing myeloid-biased and non-myeloid-biased unstimulated LTs), yielding an unstimulated myeloid-biased LT signature.

TF motif analysis—Enhancers from diverse mouse blood cells (Lara-Astiaso et al., 2014) were associated with neighboring genes with GREAT (McLean et al., 2010) and each was scanned for the mouse and (when mouse was not available) human TF motifs from CIS-BP (Weirauch et al., 2014) using an implementation of GOMER (Granek and Clarke, 2005), yielding a TF binding score for each TF/enhancer pair. TFs that distinguish cell subsets were defined as those that best discriminate between enhancers associated with genes that are specific to the subset compared to enhancers that are associated with non-specific, but expressed genes using the Wilcoxon rank sum test, yielding an enrichment score (AUROC) and P-value. P-values were subsequently corrected for multiple hypothesis testing with FDR correction, considering only those with FDR < 0.1 for subsequent analysis.

Statistical tests—All statistical analysis for the phenotypic data was done in Graphpad Prism software using an unpaired Student's T test, or a 1-way or 2-way ANOVA. Data is reported as mean ± SEM (statistical test is depicted in each figure legend). Significance measurements were marked as follows: * $p < 0.05$, ** $p < 0.01$, *** $p < 0.001$, or ns for not significant. P-values were corrected for multiple hypothesis testing by Bonferroni's multiple comparison test.

Replicate information is indicated in the figure legends.

Supplementary Material

Refer to Web version on PubMed Central for supplementary material.

Acknowledgements

This work was supported by the Sackler Foundation (D.B.), the Howard Hughes Medical Institute (A.R.), the Klaman Cell Observatory at the Broad Institute (A.R.), the Human Frontiers Science Foundation (M.M.), the National Research Service Award CA183220 (A.M), and the UCLA/Caltech Medical Scientist Training Program (A.M), the Canadian Institutes for Health Research (C.G.D), and Charles A. King Trust Postdoctoral Research Fellowship Program, Bank of America, N.A., Co-Trustee and the Simeon J. Fortin Charitable Foundation, Bank of America, N.A. (M.S.K.).

References

Akunuru S, and Geiger H (2016). Aging, Clonality, and Rejuvenation of Hematopoietic Stem Cells. Trends Mol. Med 22, 701–712. [PubMed: 27380967]

Amit I, Garber M, Chevrier N, Leite AP, Donner Y, Eisenhaure T, Guttman M, Grenier JK, Li W, Zuk O, et al. (2009). Unbiased Reconstruction of a Mammalian Transcriptional Network Mediating Pathogen Responses. Science 326, 257–263. [PubMed: 19729616]

Baldridge MT, King KY, Boles NC, Weksberg DC, and Goodell MA (2010). Quiescent haematopoietic stem cells are activated by IFN-gamma in response to chronic infection. Nature 465, 793–797. [PubMed: 20535209]

Beerman I, Bhattacharya D, Zandi S, Sigvardsson M, Weissman IL, Bryder D, and Rossi DJ (2010). Functionally distinct hematopoietic stem cells modulate hematopoietic lineage potential during aging by a mechanism of clonal expansion. Proc. Natl. Acad. Sci. U. S. A 107, 5465–5470. [PubMed: 20304793]

Benz C, Copley MR, Kent DG, Wohrer S, Cortes A, Aghaeepour N, Ma E, Mader H, Rowe K, Day C, et al. (2012). Hematopoietic stem cell subtypes expand differentially during development and display distinct lymphopoietic programs. Cell Stem Cell 10, 273–283. [PubMed: 22385655]

Bernitz JM, Kim HS, MacArthur B, Sieburg H, and Moore K (2016). Hematopoietic Stem Cells Count and Remember Self-Renewal Divisions. Cell 167, 1296–1309.e10. [PubMed: 27839867]

Bhatt DM, Pandya-Jones A, Tong A-J, Barozzi I, Lissner MM, Natoli G, Black DL, and Smale ST (2012). Transcript Dynamics of Proinflammatory Genes Revealed by Sequence Analysis of Subcellular RNA Fractions. Cell 150, 279–290. [PubMed: 22817891]

Cabezas-Wallscheid N, Klimmeck D, Hansson J, Lipka DB, Reyes A, Wang Q, Weichenhan D, Lier A, von Paleske L, Renders S, et al. (2014). Identification of regulatory networks in HSCs and their immediate progeny via integrated proteome, transcriptome, and DNA methylome analysis. Cell Stem Cell 15, 507–522. [PubMed: 25158935]

Chung NC, and Storey JD (2015). Statistical significance of variables driving systematic variation in high-dimensional data. Bioinformatics 31, 545–554. [PubMed: 25336500]

Colmegna I, Diaz-Borjon A, Fujii H, Schaefer L, Goronzy JJ, and Weyand CM (2008). Defective proliferative capacity and accelerated telomeric loss of hematopoietic progenitor cells in rheumatoid arthritis. Arthritis Rheum. 58, 990–1000. [PubMed: 18383391]

Denkinger MD, Leins H, Schirmbeck R, Florian MC, and Geiger H (2015). HSC Aging and Senescent Immune Remodeling. Trends Immunol. 36, 815–824. [PubMed: 26611154]

Dykstra B, Kent D, Bowie M, McCaffrey L, Hamilton M, Lyons K, Lee S-J, Brinkman R, and Eaves C (2007). Long-Term Propagation of Distinct Hematopoietic Differentiation Programs In Vivo. Cell Stem Cell 1, 218–229. [PubMed: 18371352]

Dykstra B, Olthof S, Schreuder J, Ritsema M, and de Haan G (2011). Clonal analysis reveals multiple functional defects of aged murine hematopoietic stem cells. J. Exp. Med 208, 2691–2703. [PubMed: 22110168]

Esplin BL, Shimazu T, Welner RS, Garrett KP, Nie L, Zhang Q, Humphrey MB, Yang Q, Borghesi LA, and Kincade PW (2011). Chronic exposure to a TLR ligand injures hematopoietic stem cells. J. Immunol 186, 5367–5375. [PubMed: 21441445]

Flach J, Bakker ST, Mohrin M, Conroy PC, Pietras EM, Reynaud D, Alvarez S, Diolaiti ME, Ugarte F, Camilla Forsberg E, et al. (2014). Replication stress is a potent driver of functional decline in ageing haematopoietic stem cells. Nature 512, 198–202. [PubMed: 25079315]

Geiger H, de Haan G, and Carolina Florian M (2013). The ageing haematopoietic stem cell compartment. Nat. Rev. Immunol 13, 376–389. [PubMed: 23584423]

Gekas C, and Graf T (2013). CD41 expression marks myeloid-biased adult hematopoietic stem cells and increases with age. Blood 121, 4463–4472. [PubMed: 23564910]

Granek JA, and Clarke ND (2005). Explicit equilibrium modeling of transcription-factor binding and gene regulation. Genome Biol. 6, R87. [PubMed: 16207358]

Grover A, Sanjuan-Pla A, Thongjuea S, Carrelha J, Giustacchini A, Gambardella A, Macaulay I, Mancini E, Luis TC, Mead A, et al. (2016). Single-cell RNA sequencing reveals molecular and functional platelet bias of aged haematopoietic stem cells. Nat. Commun 7, 11075. [PubMed: 27009448]

Haas S, Hansson J, Klimmeck D, Loeffler D, Velten L, Uckelmann H, Wurzer S, Prendergast ÁM, Schnell A, Hexel K, et al. (2015). Inflammation-Induced Emergency Megakaryopoiesis Driven by Hematopoietic Stem Cell-like Megakaryocyte Progenitors. Cell Stem Cell 17, 422–434. [PubMed: 26299573]

Hao S, and Baltimore D (2009). The stability of mRNA influences the temporal order of the induction of genes encoding inflammatory molecules. Nat. Immunol 10, 281–288. [PubMed: 19198593]

Jiang J, Chan Y-S, Loh Y-H, Cai J, Tong G-Q, Lim C-A, Robson P, Zhong S, and Ng H-H (2008). A core Klf circuitry regulates self-renewal of embryonic stem cells. Nat. Cell Biol 10, 353–360. [PubMed: 18264089]

Jovanovic M, Rooney MS, Mertins P, Przybylski D, Chevrier N, Satija R, Rodriguez EH, Fields AP, Schwartz S, Raychowdhury R, et al. (2015). Immunogenetics. Dynamic profiling of the protein life cycle in response to pathogens. Science 347, 1259038. [PubMed: 25745177]

Kharchenko PV, Silberstein L, and Scadden DT (2014). Bayesian approach to single-cell differential expression analysis. Nat. Methods 11, 740–742. [PubMed: 24836921]

Khurana S, Schouteden S, Manesia JK, Santamaria-Martínez A, Huelsken J, Lacy-Hulbert A, and Verfaillie CM (2016). Outside-in integrin signalling regulates haematopoietic stem cell function via Periostin-Itgav axis. Nat. Commun 7, 13500. [PubMed: 27905395]

King KY, and Goodell MA (2011). Inflammatory modulation of HSCs: viewing the HSC as a foundation for the immune response. Nat. Rev. Immunol 11, 685–692. [PubMed: 21904387]

Kortylewski M, Kujawski M, Herrmann A, Yang C, Wang L, Liu Y, Salcedo R, and Yu H (2009). Toll-like receptor 9 activation of signal transducer and activator of transcription 3 constrains its agonist-based immunotherapy. Cancer Res. 69, 2497–2505. [PubMed: 19258507]

Kovtonyuk LV, Fritsch K, Feng X, Manz MG, and Takizawa H (2016). Inflamm-Aging of Hematopoiesis, Hematopoietic Stem Cells, and the Bone Marrow Microenvironment. Front. Immunol7, 502. [PubMed: 27895645]

Kowalczyk MS, Tirosh I, Heckl D, Rao TN, Dixit A, Haas BJ, Schneider RK, Wagers AJ, Ebert BL, and Regev A (2015). Single-cell RNA-seq reveals changes in cell cycle and differentiation programs upon aging of hematopoietic stem cells. Genome Res. 25, 1860–1872. [PubMed: 26430063]

Lara-Astiaso D, Weiner A, Lorenzo-Vivas E, Zaretsky I, Jaitin DA, David E, Keren-Shaul H, Mildner A, Winter D, Jung S, et al. (2014). Immunogenetics. Chromatin state dynamics during blood formation. Science 345, 943–949. [PubMed: 25103404]

Li B, and Dewey CN (2011). RSEM: accurate transcript quantification from RNA-Seq data with or without a reference genome. BMC Bioinformatics 12, 323. [PubMed: 21816040]

Mantel C, Messina-Graham S, Moh A, Cooper S, Hangoc G, Fu X-Y, and Broxmeyer HE (2012). Mouse hematopoietic cell-targeted STAT3 deletion: stem/progenitor cell defects, mitochondrial dysfunction, ROS overproduction, and a rapid aging-like phenotype. Blood 120, 2589–2599. [PubMed: 22665934]

Mayr C, and Bartel DP (2009). Widespread shortening of 3'UTRs by alternative cleavage and polyadenylation activates oncogenes in cancer cells. Cell 138, 673–684. [PubMed: 19703394]

McLean CY, Bristor D, Hiller M, Clarke SL, Schaar BT, Lowe CB, Wenger AM, and Bejerano G (2010). GREAT improves functional interpretation of cis-regulatory regions. Nat. Biotechnol 28, 495–501. [PubMed: 20436461]

Mehta A, Zhao JL, Sinha N, Marinov GK, Mann M, Kowalczyk MS, Galimidi RP, Du X, Erikci E, Regev A, et al. (2015). The MicroRNA-132 and MicroRNA-212 Cluster Regulates Hematopoietic Stem Cell Maintenance and Survival with Age by Buffering FOXO3 Expression. Immunity 42, 1021–1032. [PubMed: 26084022]

Morita Y, Ema H, and Nakauchi H (2010). Heterogeneity and hierarchy within the most primitive hematopoietic stem cell compartment. J. Exp. Med. 207, 1173–1182. [PubMed: 20421392]

Mossadegh-Keller N, Sarrazin S, Kandalla PK, Espinosa L, Stanley ER, Nutt SL, Moore J, and Sieweke MH (2013). M-CSF instructs myeloid lineage fate in single haematopoietic stem cells. Nature 497, 239–243. [PubMed: 23575636]

Nagai Y, Garrett KP, Ohta S, Bahrun U, Kouro T, Akira S, Takatsu K, and Kincade PW (2006). Toll-like receptors on hematopoietic progenitor cells stimulate innate immune system replenishment. Immunity 24, 801–812. [PubMed: 16782035]

Nemeth JA, Nakada MT, Trikha M, Lang Z, Gordon MS, Jayson GC, Corringham R, Prabhakar U, Davis HM, and Beckman RA (2007). Alpha-v integrins as therapeutic targets in oncology. Cancer Invest. 25, 632–646. [PubMed: 18027153]

Ng SY-M, Yoshida T, Zhang J, and Georgopoulos K (2009). Genome-wide lineage-specific transcriptional networks underscore Ikaros-dependent lymphoid priming in hematopoietic stem cells. Immunity 30, 493–507. [PubMed: 19345118]

Novershtern N, Subramanian A, Lawton LN, Mak RH, Haining WN, McConkey ME, Habib N, Yosef N, Chang CY, Shay T, et al. (2011). Densely interconnected transcriptional circuits control cell states in human hematopoiesis. Cell 144, 296–309. [PubMed: 21241896]

O'Connell RM, et al. (2010). MicroRNAs enriched in hematopoietic stem cells differentially regulate long-term hematopoietic output. Proc Natl Acad Sci U S A 107(32), 14235–40. [PubMed: 20660734]

Pang WW, Price EA, Sahoo D, Beerman I, Maloney WJ, Rossi DJ, Schrier SL, and Weissman IL (2011). Human bone marrow hematopoietic stem cells are increased in frequency and myeloid-biased with age. Proc. Natl. Acad. Sci. U. S. A 108, 20012–20017. [PubMed: 22123971]

Picelli S, Björklund ÅK, Faridani OR, Sagasser S, Winberg G, and Sandberg R (2013). Smart-seq2 for sensitive full-length transcriptome profiling in single cells. Nat. Methods10, 1096–1098. [PubMed: 24056875]

Pietras EM, Reynaud D, Kang Y-A, Carlin D, Calero-Nieto FJ, Leavitt AD, Stuart JM, Göttgens B, and Passegué E (2015). Functionally Distinct Subsets of Lineage-Biased Multipotent Progenitors Control Blood Production in Normal and Regenerative Conditions. Cell Stem Cell 17, 35–46. [PubMed: 26095048]

Ramirez-Carrozzi VR, Braas D, Bhatt DM, Cheng CS, Hong C, Doty KR, Black JC, Hoffmann A, Carey M, and Smale ST (2009). A unifying model for the selective regulation of inducible transcription by CpG islands and nucleosome remodeling. Cell 138, 114–128. [PubMed: 19596239]

Robinson MD, McCarthy DJ, and Smyth GK (2010). edgeR: a Bioconductor package for differential expression analysis of digital gene expression data. Bioinformatics 26, 139–140. [PubMed: 19910308]

Sanjuan-Pla A, Macaulay IC, Jensen CT, Woll PS, Luis TC, Mead A, Moore S, Carella C, Matsuoka S, Bouriez Jones T, et al. (2013). Platelet-biased stem cells reside at the apex of the haematopoietic stem-cell hierarchy. Nature 502, 232–236. [PubMed: 23934107]

Rossi DJ, Bryder D, Zahn JM, Ahlenius H, Sonu R, Wagers AJ, and Weissman IL (2005). Cell intrinsic alterations underlie hematopoietic stem cell aging. Proc. Natl. Acad. Sci. U. S. A 102,

Sawai CM, Babovic S, Upadhaya S, Knapp DJHF, Lavin Y, Lau CM, Goloborodko A, Feng J, Fujisaki J, Ding L, et al. (2016). Hematopoietic Stem Cells Are the Major Source of Multilineage Hematopoiesis in Adult Animals. Immunity 45, 597–609. [PubMed: 27590115]

Shahrin NH, Diakiw S, Dent LA, Brown AL, and D'Andrea RJ (2016). Conditional knockout mice demonstrate function of Klf5 as a myeloid transcription factor. Blood 128, 55–59. [PubMed: 27207790]

Shattil SJ, Kashiwagi H, and Pampori N (1998). Integrin signaling: the platelet paradigm. Blood 91, 2645–2657. [PubMed: 9531572]

Sudo K, Ema H, Morita Y, and Nakauchi H (2000). Age-associated characteristics of murine hematopoietic stem cells. J. Exp. Med 192, 1273–1280. [PubMed: 11067876]

Sun D, Luo M, Jeong M, Rodriguez B, Xia Z, Hannah R, Wang H, Le T, Faull KF, Chen R, et al. (2014). Epigenomic Profiling of Young and Aged HSCs Reveals Concerted Changes during Aging that Reinforce Self-Renewal. Cell Stem Cell 14, 673–688. [PubMed: 24792119]

Tanay A, and Regev A (2017). Scaling single-cell genomics from phenomenology to mechanism. Nature 541, 331–338. [PubMed: 28102262]

Taniguchi Ishikawa E, Chang KH, Nayak R, Olsson HA, Ficker AM, Dunn SK, Madhu MN, Sengupta A, Whitsett JA, Grimes HL, et al. (2013). Klf5 controls bone marrow homing of stem cells and progenitors through Rab5-mediated β1/β2-integrin trafficking. Nat. Commun 4, 1660. [PubMed: 23552075]

Umemoto T, Yamato M, Shiratsuchi Y, Terasawa M, Yang J, Nishida K, Kobayashi Y, and Okano T (2006). Expression of Integrin beta3 is correlated to the properties of quiescent hemopoietic stem cells possessing the side population phenotype. J. Immunol 177, 7733–7739. [PubMed: 17114444]

Umemoto T, Yamato M, Shiratsuchi Y, Terasawa M, Yang J, Nishida K, Kobayashi Y, and Okano T (2008). CD61 enriches long-term repopulating hematopoietic stem cells. Biochem. Biophys. Res. Commun 365, 176–182. [PubMed: 17983596]

Wagner A, Regev A, and Yosef N (2016). Revealing the vectors of cellular identity with single-cell genomics. Nat. Biotechnol 34, 1145–1160. [PubMed: 27824854]

Wang J, Sun Q, Morita Y, Jiang H, Gross A, Lechel A, Hildner K, Guachalla LM, Gompf A, Hartmann D, et al. (2012). A differentiation checkpoint limits hematopoietic stem cell self-renewal in response to DNA damage. Cell 148, 1001–1014. [PubMed: 22385964]

Weirauch MT, Yang A, Albu M, Cote AG, Montenegro-Montero A, Drewe P, Najafabadi HS, Lambert SA, Mann I, Cook K, et al. (2014). Determination and inference of eukaryotic transcription factor sequence specificity. Cell 158, 1431–1443. [PubMed: 25215497]

Wunder EW, and Henon PR (2012). Peripheral Blood Stem Cell Autografts (Springer Science & Business Media).

Yamamoto R, Morita Y, Ooehara J, Hamanaka S, Onodera M, Rudolph KL, Ema H, and Nakauchi H (2013). Clonal analysis unveils self-renewing lineage-restricted progenitors generated directly from hematopoietic stem cells. Cell 154, 1112–1126. [PubMed: 23993099]

Yamamoto R, Wilkinson AC, Ooehara J, Lan X, Lai C-Y, Nakauchi Y, Pritchard JK, and Nakauchi H (2018). Large-Scale Clonal Analysis Resolves Aging of the Mouse Hematopoietic Stem Cell Compartment. Cell Stem Cell 22, 600–607.e4. [PubMed: 29625072]

Young K, Borikar S, Bell R, Kuffler L, Philip V, and Trowbridge JJ (2016). Progressive alterations in multipotent hematopoietic progenitors underlie lymphoid cell loss in aging. J. Exp. Med 213, 2259–2267. [PubMed: 27811054]

Yu VWC, Yusuf RZ, Oki T, Wu J, Saez B, Wang X, Cook C, Baryawno N, Ziller MJ, Lee E, et al. (2016). Epigenetic Memory Underlies Cell-Autonomous Heterogeneous Behavior of Hematopoietic Stem Cells. Cell 167, 1310–1322.e17. [PubMed: 27863245]

Zhao JL, Rao DS, Boldin MP, Taganov KD, O'Connell RM, and Baltimore D (2011). NF-kappaB dysregulation in microRNA-146a-deficient mice drives the development of myeloid malignancies. Proc. Natl. Acad. Sci. U. S. A 108, 9184–9189. [PubMed: 21576471]

Zhao JL, Rao DS, O'Connell RM, Garcia-Flores Y, and Baltimore D (2013). MicroRNA-146a acts as a guardian of the quality and longevity of hematopoietic stem cells in mice. Elife 2.

Zhao JL, Ma C, O'Connell RM, Mehta A, DiLoreto R, Heath JR, and Baltimore D (2014). Conversion of danger signals into cytokine signals by hematopoietic stem and progenitor cells for regulation of stress-induced hematopoiesis. Cell Stem Cell 14, 445–459. [PubMed: 24561084]

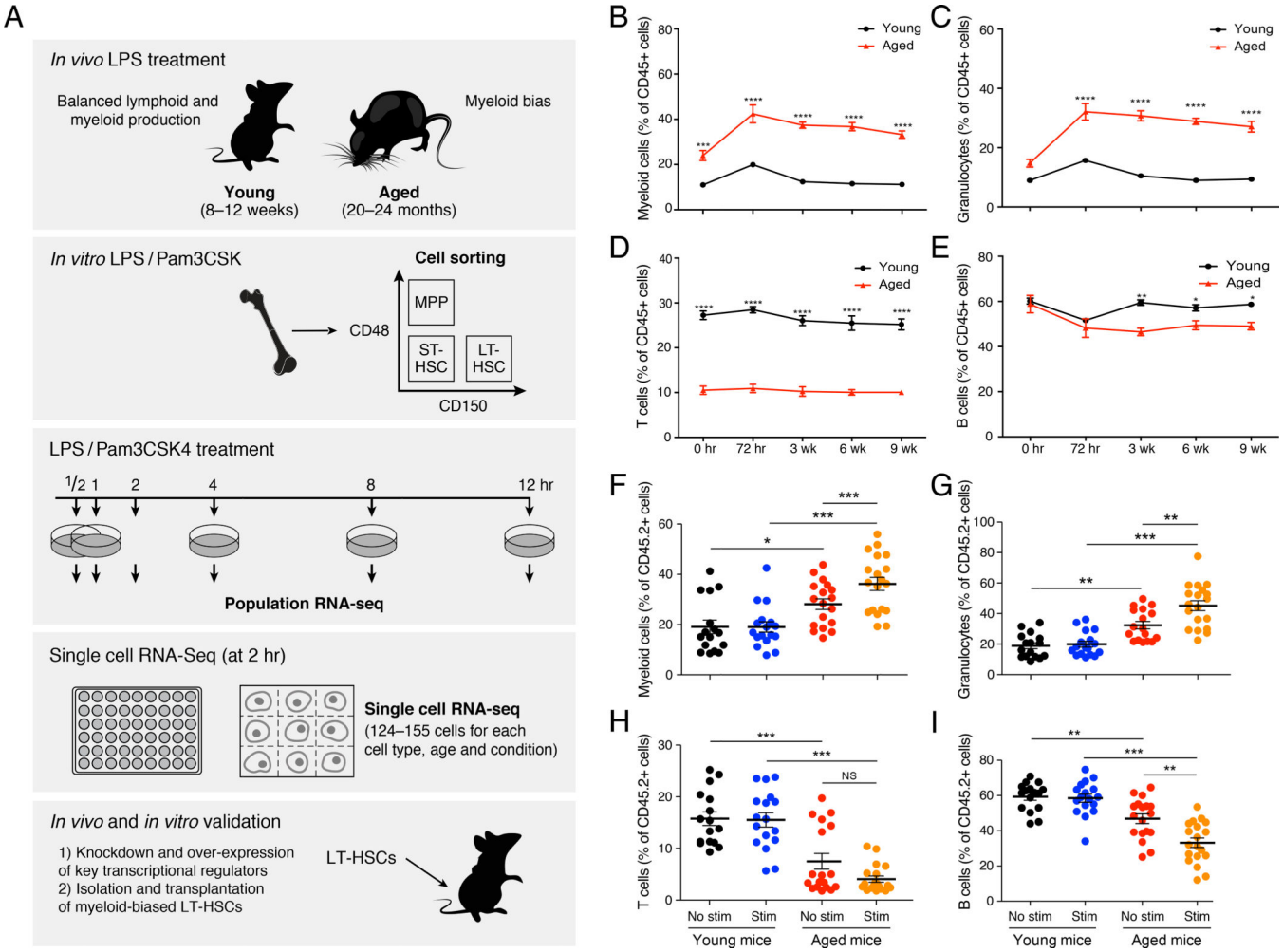

Figure 1. Aged hematopoietic stem cells exposed to inflammatory signals demonstrate increased myeloid output in a cell-intrinsic manner.

(A) Schematic overview of the approach. (B)-(E) Young and aged mice were exposed to a second dose of LPS 1 month after the initial LPS challenge and the frequency of (B) CD11b+, (C) Gr-1+, (D) CD3+, and (E) CD19+ was observed for 9 weeks. (F)-(I) LT-HSCs sorted from young and aged CD45.2 mice were stimulated with LPS and Pam3csk4 for 2 hours prior to competitive transplant into CD45.1 recipients. Peripheral blood CD45.2 (F) CD11b+, (G) Gr-1+, (H) CD3+ and (I) CD19+ frequencies were measured by flow cytometry at 3 months post-reconstitution (n = 11–12 per group). Data represent at least two independent experiments and are presented as mean ± SEM. * denotes $p < 0.05$, ** denotes $p < 0.01$ and *** denotes $p < 0.001$. P-values were corrected for multiple hypothesis testing by Bonferroni's multiple comparison test.

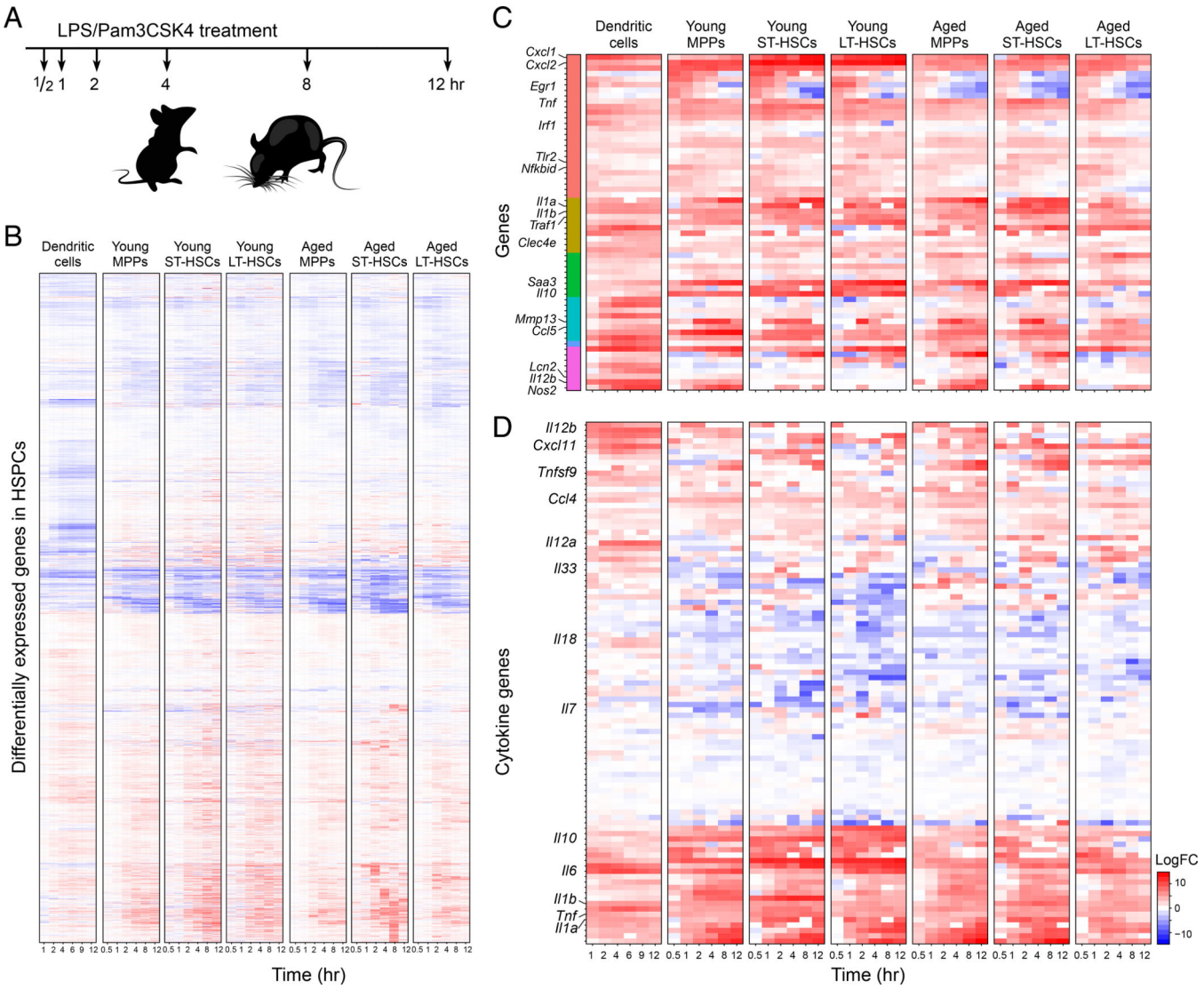

Figure 2. Early hematopoietic progenitors demonstrate a rapid transcriptional response to inflammatory signals.

(A) Schematic of LPS and Pam3CSK4 time-course experiment. LT-HSCs, ST-HSCs and MPPs from 5 young and 5 aged mice were exposed to LPS and Pam3CSK4 *in vitro* for the indicated time after which RNA was harvested for bulk RNA-sequencing. (B) Heatmap of differentially expressed genes in young and aged hematopoietic progenitors alongside an expression map of mature bone-marrow derived dendritic cells (DCs) challenged with LPS for comparison. (C) Heatmap of NF-kB regulated inflammatory genes clustered by temporal expression patterns described previously. (D) Heatmap of cytokines expressed in early progenitors and DCs.

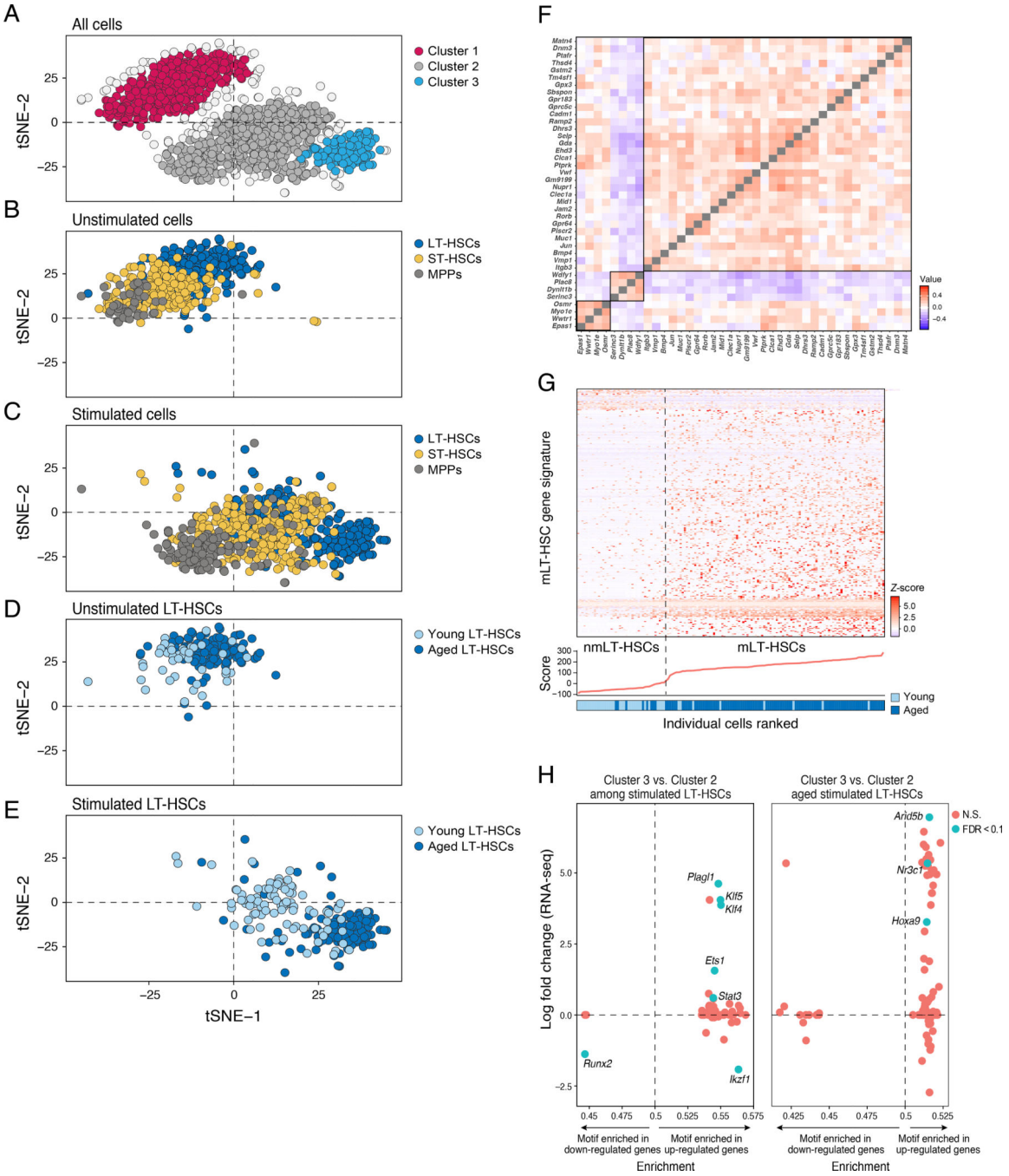

Figure 3. Single-cell RNA-sequencing reveals heterogeneity in the hematopoietic stem cell compartment that is altered with age.

(A)-(E) LT-HSCs, ST-HSCs and MPPs from 5 young and 4 aged mice were stimulated with LPS and Pam3CSK4 and sorted for scRNA-seq. scRNA-seq data for all cells, projected on two t-SNE axes. (A) Density-based clusters. (B)-(E) Single-cell t-SNE plots (as before) indicating all cell types among (B) unstimulated and (C) stimulated cells, and mouse ages among (D) unstimulated and (E) stimulated LT-HSCs. (F) Correlation across cells between DE genes common to both simulated cluster 3 vs 2 and unstimulated aged vs young LT-HSCs. Three clusters of correlated genes are identified. (G) Heat-map represents the

expression values of genes in the unstimulated myeloid-biased gene signature for each single unstimulated LT-HSC. The panels below show the myeloid signature score for each cell and is the basis for the ordering of the x axis. The bottom color-coded bar shows the age of the animals from which the cells were derived. (H) Enrichment of transcription factor motifs in enhancers of cluster 3-vs-2-specific genes for all cells (left), or only aged LT-HSCs (right) (x-axis) and differential expression of the TF genes themselves in the same comparison (y-axis). Significant genes (FDR<0.1) are indicated. An enrichment score > 0.5 indicates that the TF motif is enriched among genes that are expressed more highly in cluster 3, while a score below 0.5 indicates that the TF is expressed more highly in cluster 2.

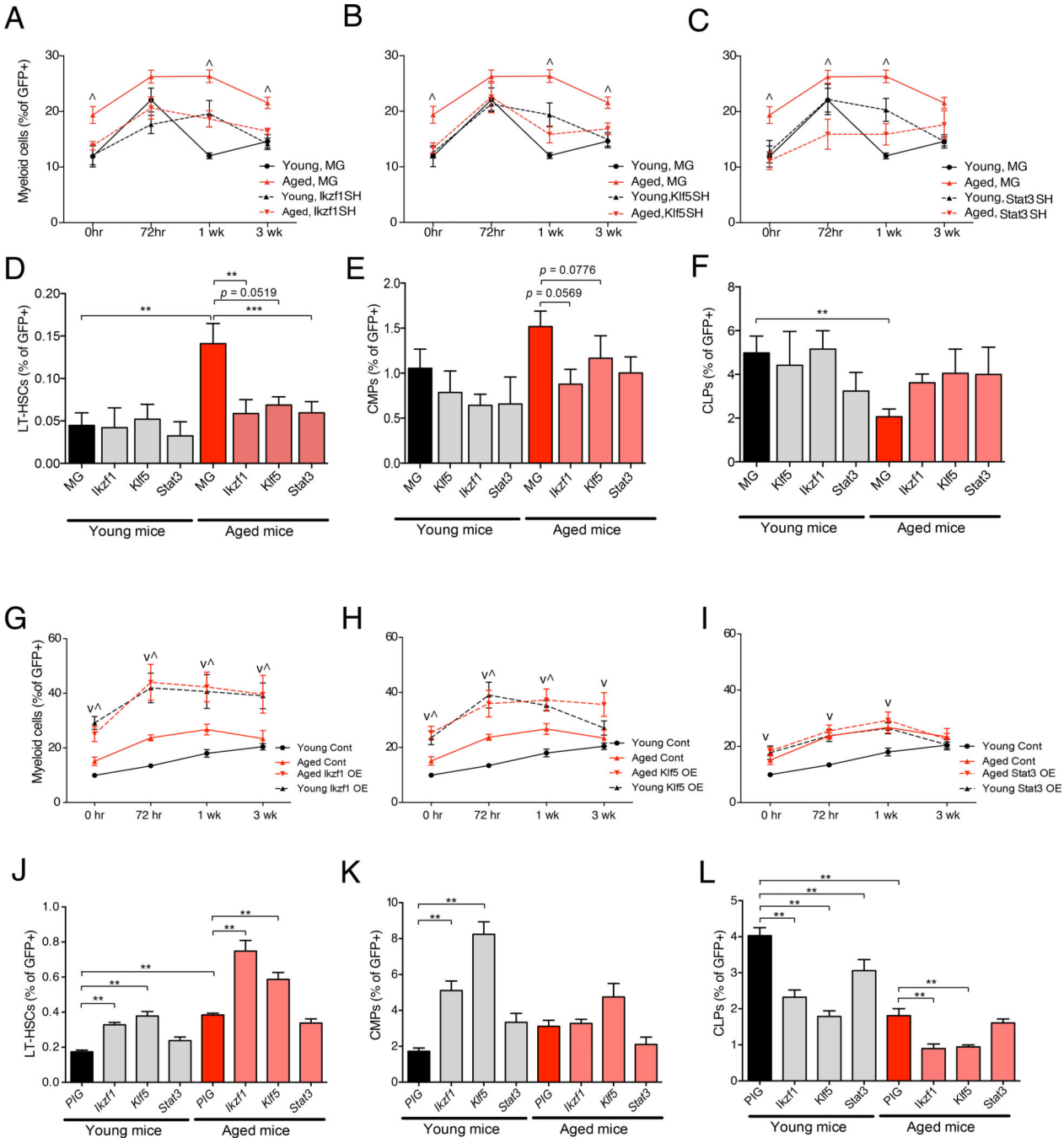

Figure 4. Klf5, Ikzf1, and Stat3 regulate steady-state and inflammatory age-related myeloid bias.

Bone marrow cells from young and aged C57BL/6 mice were transduced with constructs to either knock-down (denoted SH in A-F), or overexpress (denoted OE in G-L) the indicated transcription factors. These cells were subsequently reconstituted into lethally irradiated young C57BL/6 recipient mice. These mice were subsequently challenged with a single sub-lethal dose of LPS and peripheral blood immune cells were tracked over time by flow cytometry. Shown are peripheral blood myeloid cells for mice with knockdown or overexpression of (A,G) Ikzf1, (B,H) Klf5, and (C,I) Stat3. These mice were subsequently

harvested and the bone marrow was analyzed for the frequency of (D,J) LT-HSCs, (E,K) CMPs, and (F,L) CLPs from knockdown and overexpression mice, respectively. Data represent at least two independent experiments (n=8–10 mice per group) and are presented as mean ± SEM. (A)-(C) and (G)-(H) ^ denotes $p<0.05$ for aged shRNA or OE vs. Aged MG, ^{v}denotes $p<0.05$ for aged shRNA or OE vs. young MG using two way ANOVA. (D-F, J-L) * denotes $p < 0.05$, ** denotes $p < 0.01$ and *** denotes $p < 0.001$. P-values was corrected for multiple hypothesis testing by Bonferroni's method.

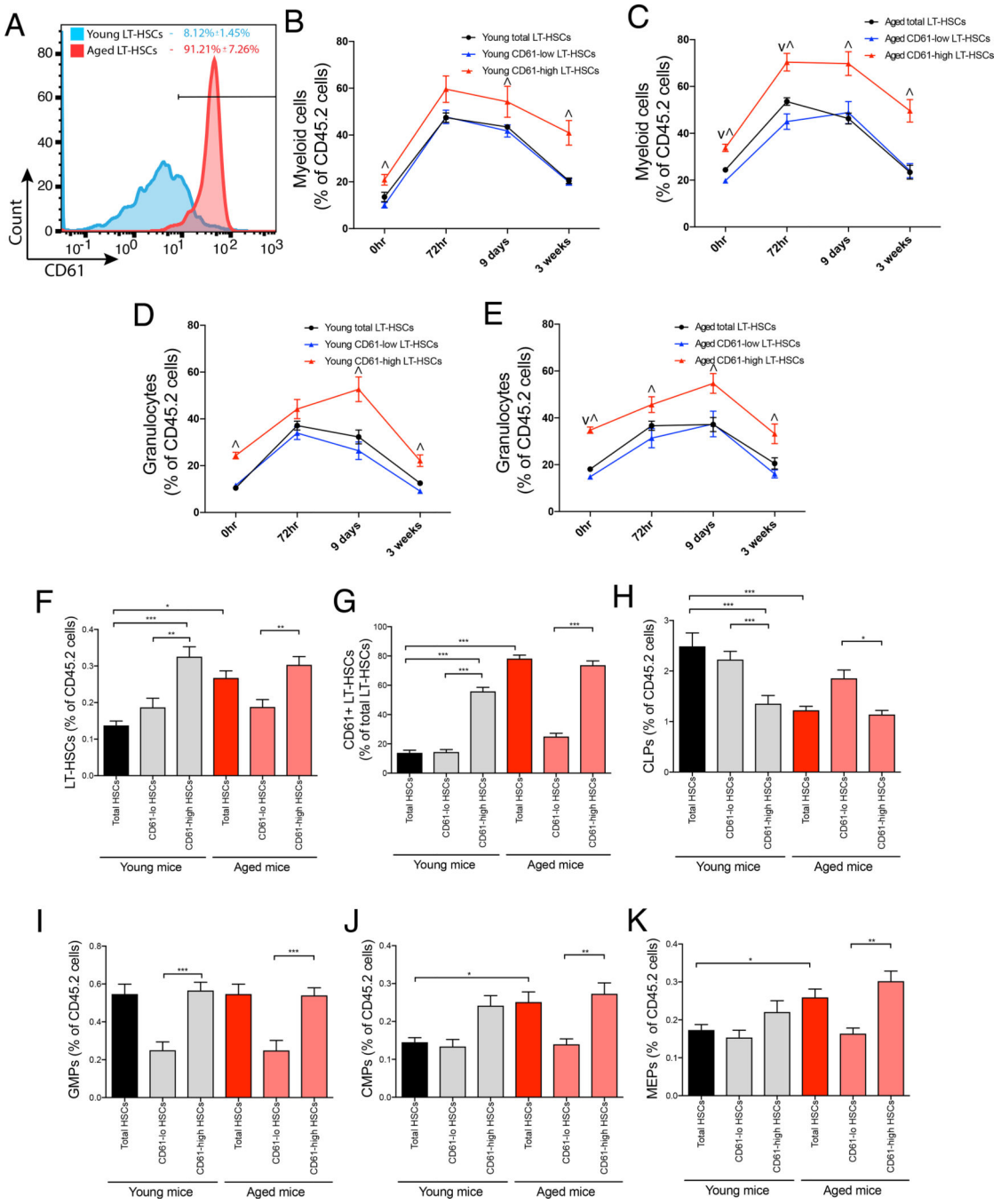

Figure 5. CD61 expression on LT-HSCs is a marker for mLT-HSCs.

(A) Flow cytometry plots showing CD61 expression in aged and young LT-HSCs. (B)-(E) Total LT-HSCs, and those with elevated (CD61-high) and decreased (CD61-low) expression of CD61, from aged and young mice were transplanted into lethally irradiated young C57BL/6 recipient mice. Mice were subsequently challenged with a single dose of LPS as in Figure 1. Shown are the peripheral blood CD11b+ cell frequencies from mice transplanted with (B) young and (C) aged donor LT-HSCs, and the peripheral blood Gr-1+ frequencies from mice transplanted with (D) young and (E) aged donor LT-HSCs. (F)-(K) Transplanted

mice were harvested at 4-months post-reconstitution. Shown are the bone marrow frequencies of (F) LT-HSCs, (G) CD61+ LT-HSCs, (H) CLPs, (I) GMPs, (J) CMPs and (K) MEPs in these mice. (A) CD61 high frequencies and SD are depicted for aged (red) and young (blue) (n=4 per group). (B-K) Data represent at least two independent experiments (n=7–12 per group) and are presented as mean ± SEM. ^ denotes $p<0.05$ for CD61-high vs. control, ^{v}denotes $p<0.05$ for CD61-low vs. control using two way ANOVA. * denotes $p < 0.05$, ** denotes $p < 0.01$ and *** denotes $p < 0.001$. P-values was corrected for multiple hypothesis testing by Bonferroni's method.

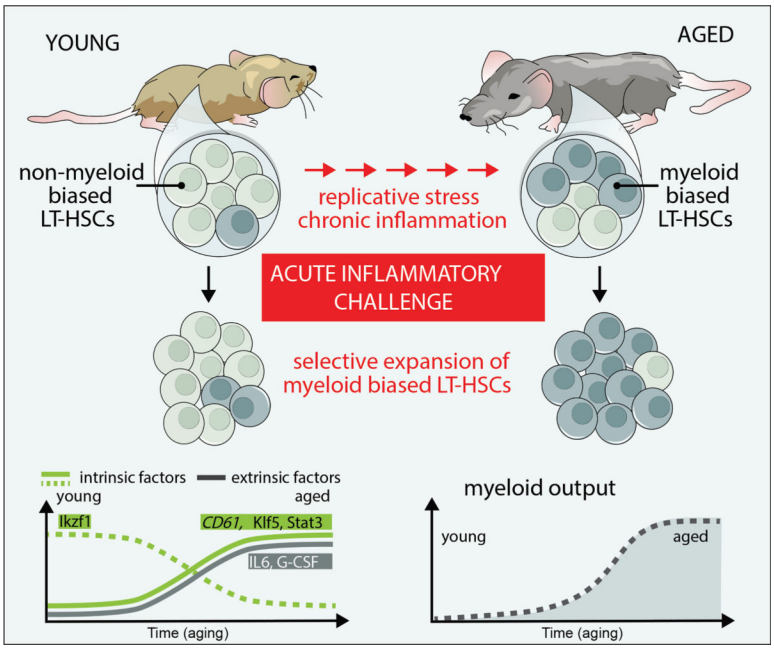

Figure 6. Model of LT-HSC aging and inflammatory myeloid-bias.

Shifts in clonal heterogeneity during LT-HSC aging affects the inflammatory response of LT-HSCs. The LT-HSC compartment is comprised of unbiased and myeloid-biased LT-HSCs. With age, the clonal distribution of LT-HSCs shifts towards myeloid-biased variants which express high levels of CD61. During acute inflammatory challenges, aged myeloid-biased LT-HSCs preferentially expand, leading to increased myeloid output. Several cell-intrinsic factors, including the transcriptional regulators Klf5, Ikzf1 and Stat3 may play a role in establishing a myeloid-biased differentiation program during aging and inflammation. Extrinsic factors, including inflammatory cytokines and growth factors secreted from other cell types may also play a role.

REAGENT or RESOURCE	SOURCE	IDENTIFIER
Antibodies		
CD11c	Biolegend	117304 N418
CD3e	Biolegend	100304 145–2C11
NK1.1	Biolegend	108704 PK136
IL-7Ra	Biolegend	135006 A7R34
Ter-119	Biolegend	116204 TER-119
CD11b	Biolegend	101204 M1/70
CD8a	Biolegend	100704 53–6.7
CD4	eBioscience	13–0041-82 gk1.5
B220	Biolegend	103204 RA3–6B2
CD19	Biolegend	115504 6D5
GR-1	Biolegend	108403 RB6–8C5
CD45.1 PE	Biolegend	110708 a20
CD45.2 eflour 450	eBioscience	48–0454-82 104
GR1 APC	Biolegend	108412 RB6–8C5
CD3E FITC	Biolegend	100306 145–2C11
CD11B PE/CY5	Biolegend	101209 M1/70
CD45.2 PE/CY5	Biolegend	25–0454-80 104
CD3E PE/CY5	eBioscience	100310 145–2C11
IL-7Ra PE/CY5	Biolegend	135016 A7R34
NK1.1 PE/CY5	Biolegend	108716 PK136
GR1 PE/CY5	Biolegend	108410 RB6–8C5
cd11B PE/CY5	Biolegend	101209 M1/70
CD19 PE/CY5	Biolegend	115510 6D5
CD4 PE/CY5	BIolegend	15–0041–82 GK1.5
TER-119 PE/CY5	EBioscience	116209 TER-119
FC BLOCK	Biolegend	101302 93
CD150 PE/CY7	Biolegend	115914 TC15–12F12.2
CD45.2 APC/CY7	Biolegend	109824 104
CD34 EFLOUR450	Biolegend	48–0341–80 RAM34
CD34 PE	EBioscience	128610 HM34
IL-7Ra PE	Biolegend	135009 A7R34
CD48 PACBLUE	Biolegend	103418 HM48–1
CD61 PE	Biolegend	12–0611–82 2C9.G3
CD38 APC/CY7	EBioscience	102728 90
CD34 APC/CY7	BIolegend	128614 HM34
CD16/32 EFLOUR450	Biolegend	48–0161–82 93
CD16/32 VIOLET 420	EBioscience	101331 93

REAGENT or RESOURCE	SOURCE	IDENTIFIER
CD16/32 PE/CY7	Biolegend	25–0161–81 93
SCA1 APC	EBioscience	108112 D7
SCA1 PACBLUE	Biolegend	108120 D7
CKIT APC	Biolegend	105812 2B8
CKIT PE	Biolegend	1335106 ACK2
CKIT FITC	Biolegend	105806 2B8
CD135 APC	Biolegend	135310 A2F10
CD41 PE	Biolegend	133906 B203323
CD51 PE	Biolegend	104106 B240646
CD61 APC	Biolegend	104316 B219725
Bacterial and Virus Strains		
PCL-ecotropic pseudotyped gamma-retrovirus	O'Connell et al. J Exp Med. 2008 Mar 17. 205(3):585–94.	Adgene: #26528
Chemicals, Peptides, and Recombinant Proteins		
LPS	SIGMA	L2880–100MG
Pam3CSK4	Invivogen	41–11–60–10
Dulbecco's Modification of Eagle's Medium	Corning	10–013-CV
Fetal Bovine Serum	Corning	35–015-CV
Penicillin Streptomycin Solution (100x)	Corning	30–002-Cl
0.25% Trypsin	Corning	25–053-Cl
TRIzol Reagent	Invitrogen	15596026
Protoscript II	New England Biolabs	M0368L
Antarctic phosphatase	New England Biolabs	M0289S
Puromycin	InvivoGen	Cat#ant-pr-1
Murine SCF	PeproTech	250–03
Murine IL-6	PeproTech	216–16
Murine IL-3	PeproTech	213–13
Critical Commercial Assays		
BioT	Bioland	B01–01
Nextera XT DNA Library Preparation Kit	illumina	FC-131–1096
qScript cDNA SuperMix	Quanta	95048–100
KAPA HiFi HotStart ReadyMix	KAPA biosystems	KM2602
Deposited Data		
RNA-Seq Gene Expression and IR Data	This Paper	GEO: GSE100428
Experimental Models: Cell Lines		
HEK293T	ATCC	CRL-3216
Experimental Models: Organisms/Strains		
Mouse: C57BL/6J	Jackson Laboratory	000664
Mouse: C57BL/6J	Charles Rivers Laboratories	C57BL/6NCrl
Oligonucleotides - source		

REAGENT or RESOURCE	SOURCE	IDENTIFIER
Primers used	Table S5	This paper
shRNA sequences	Table S5	This paper
cDNA sequences for transcription factors over expression	Table S5	This paper